SPIE Optics & Photonics, 14 August 2019

Polarization Effects Modeling with Field Tracing

Site Zhang[1], Christian Hellmann[2], and Frank Wyrowski[3]

[1] LightTrans International UG

[2] Wyrowski Photonics GmbH

[3] Applied Computational Optics Group, Friedrich-Schiller-Universität Jena

SPIE Optics & Photonics, 14 August 2019

Polarization Effects Modeling with Field Tracing

Site Zhang[1], Christian Hellmann[2], and Frank Wyrowski[3]

[1] **LightTrans International UG**
[2] Wyrowski Photonics GmbH
[3] Applied Computational Optics Group, Friedrich-Schiller-Universität Jena

Jena, Germany

LightTrans International

LightTrans
- Distribution of VirtualLab Fusion, together with distributors worldwide
- Technical support, seminars, and trainings
- Engineering projects

University of Jena

Applied Computational Optics Group R&D in optical modeling and design with emphasis on physical optics

Wyrowski Photonics

Wyrowski Photonics
Development of fast physical optics software VirtualLab Fusion

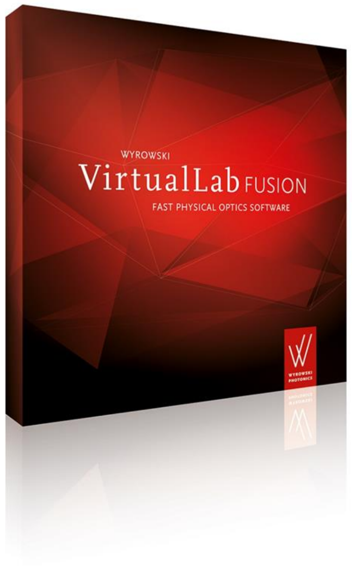

Optical Design Software and Services

Booth #110

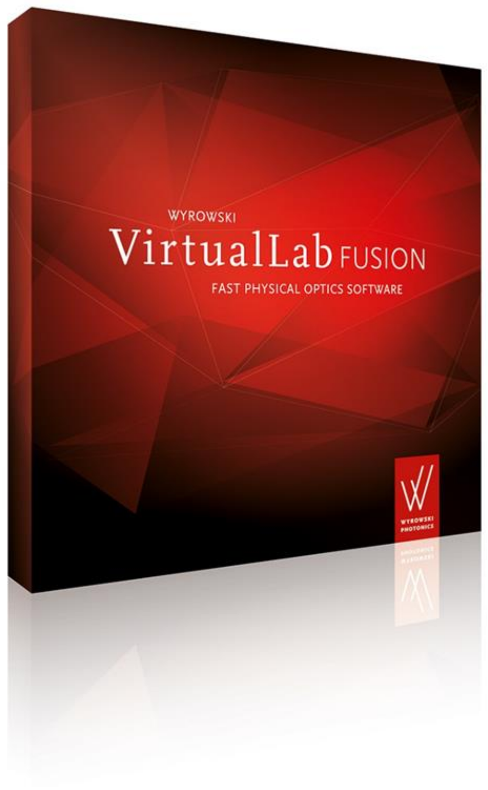

Motivation

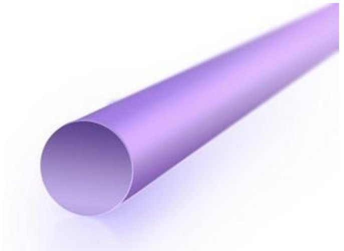

YAG crystal rod
(http://www.altechna.com)

BBO crystal slabs
(http://www.altechna.com)

- Stress-induced birefringence in laser crystals

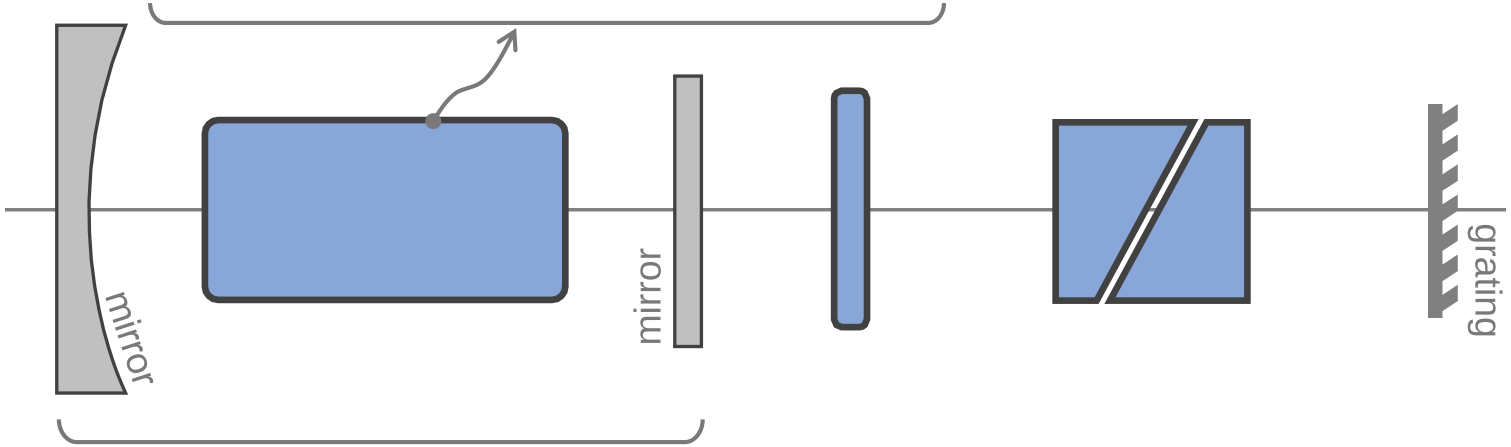

- Laser cavity with crystal for vector beam generation

Motivation

Polarizers / Waveplates
(http://www.altechna.com)

- Polarizer and its model for non-paraxial cases

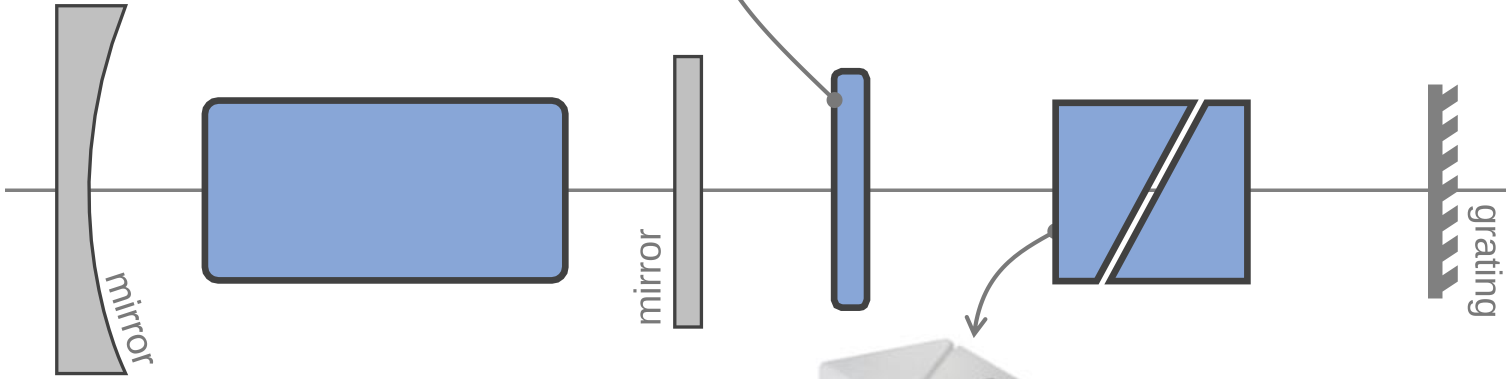

Wollaston prism
(https://www.thorlabs.com)

- Prisms made out of birefringent materials

Motivation

- Optical birefringence / anisotropy, either desired or detrimental, is present in many optical systems
- Such effects have influences on polarization and play a role in polarization manipulation

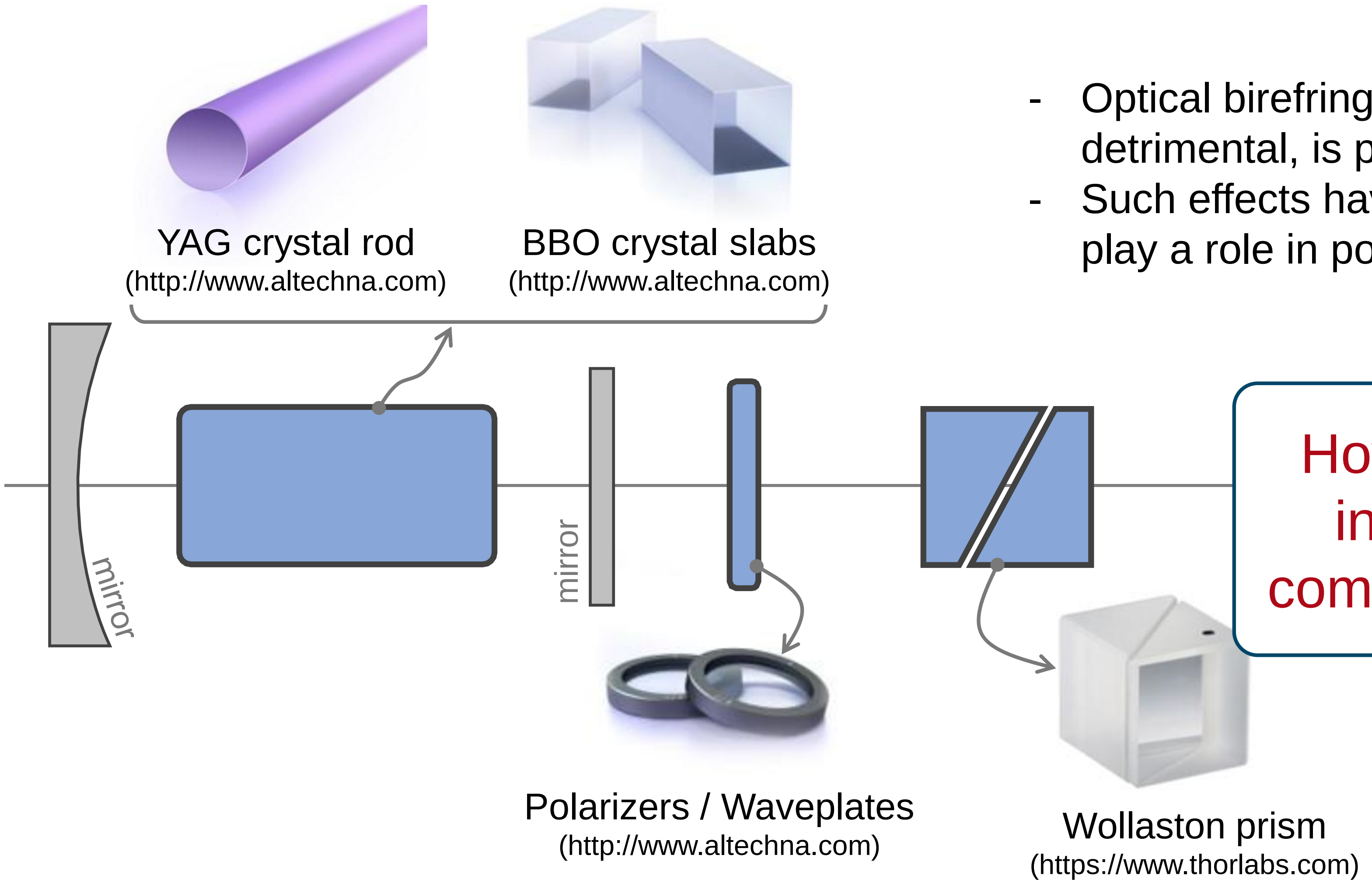

How to take **birefringence** into consideration within complete **system modeling**?

Scope of This Work

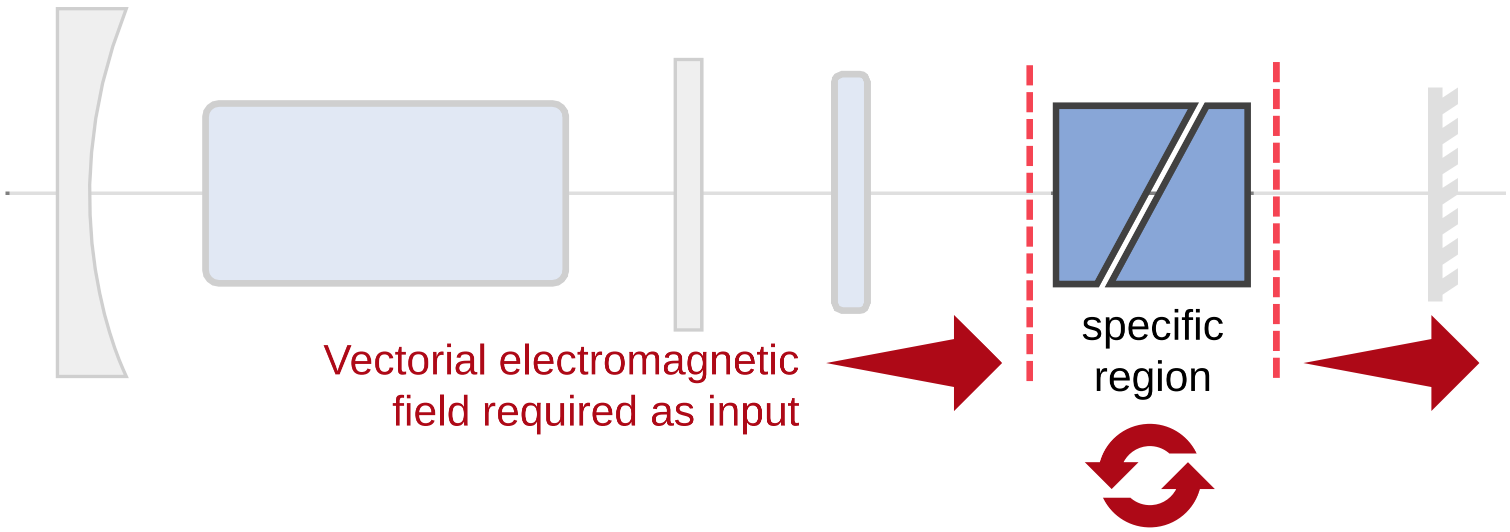

Vectorial electromagnetic field required as input

Output vectorial field delivered with birefringence influence
(also prepared for subsequent components)

Interaction with components including birefringence

Modeling must be based on **electromagnetic fields**!

Field Tracing Concept

F. Wyrowski and M. Kuhn, “Introduction to field tracing,” Journal of Modern Optics **58**, 449-466 (2011)

M. Kuhn, F. Wyrowski, and C. Hellmann, “Non-sequential optical field tracing,” in *Advanced Finite Element Methods and Applications,* by T. Apel and O. Steinbach. Vol. **66**, 257–273 (2013)

F. Wyrowski, “Unification of the geometric and diffractive theories of electromagnetic fields,” Proc. DGaO (2017).

Single Solver for Complete System?

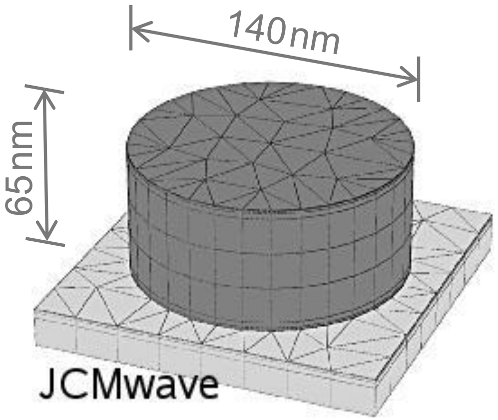

Finite element method (FEM) analysis of a silver nano-disc
www. jcmwave.com

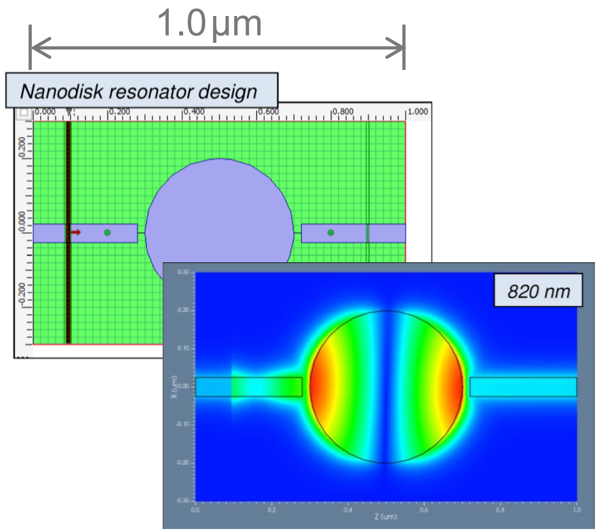

Plasmonic waveguide filters with nanodisk resonators, FDTD simulation
www.optiwave.com

Single Solver for Complete System?

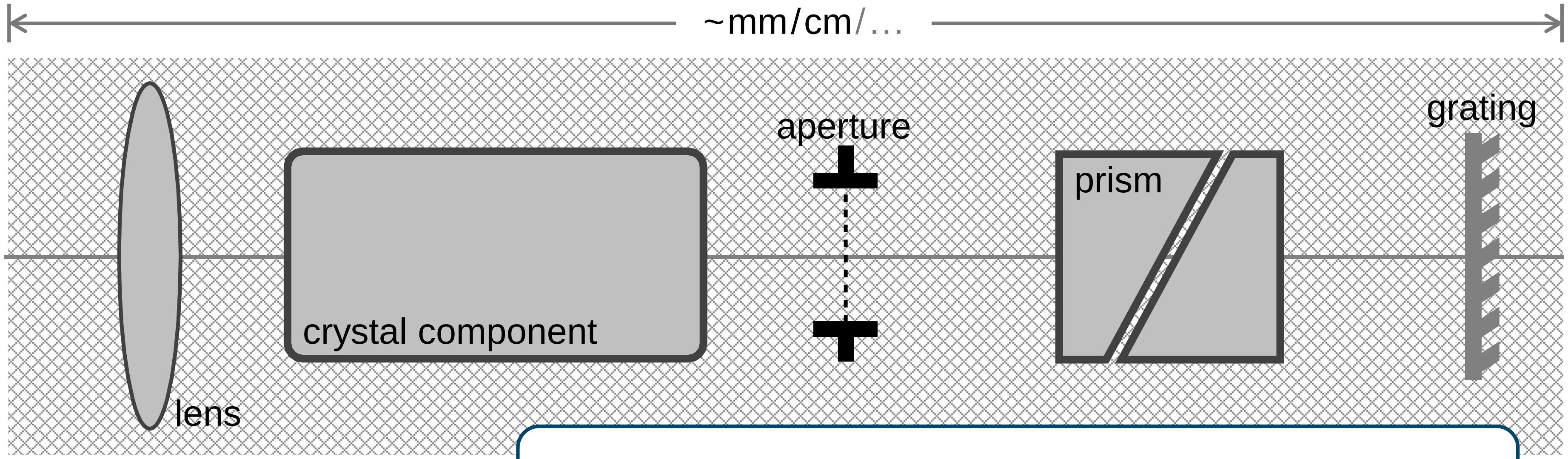

A single rigorous method (e.g. FEM, FDTD) is often numerically **infeasible** to model a complete optical system

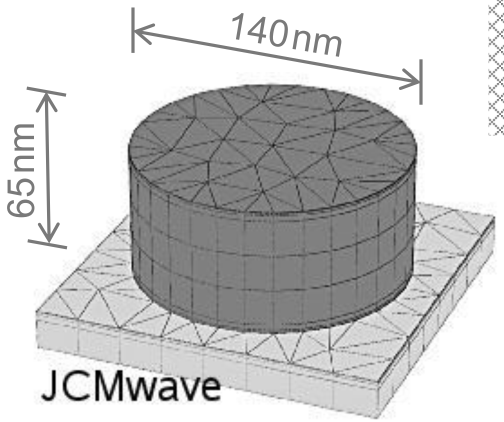

Finite element method (FEM) analysis of a silver nano-disc
www. jcmwave.com

Field Tracing – Connecting Field Solvers

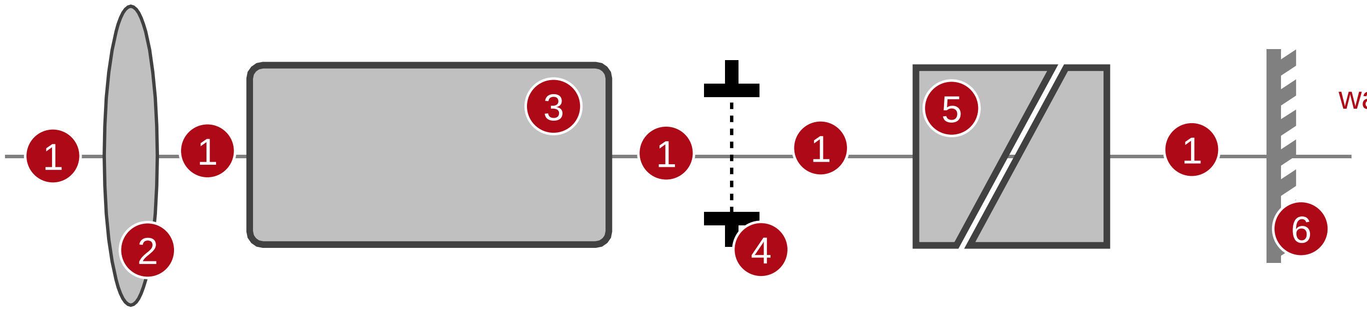

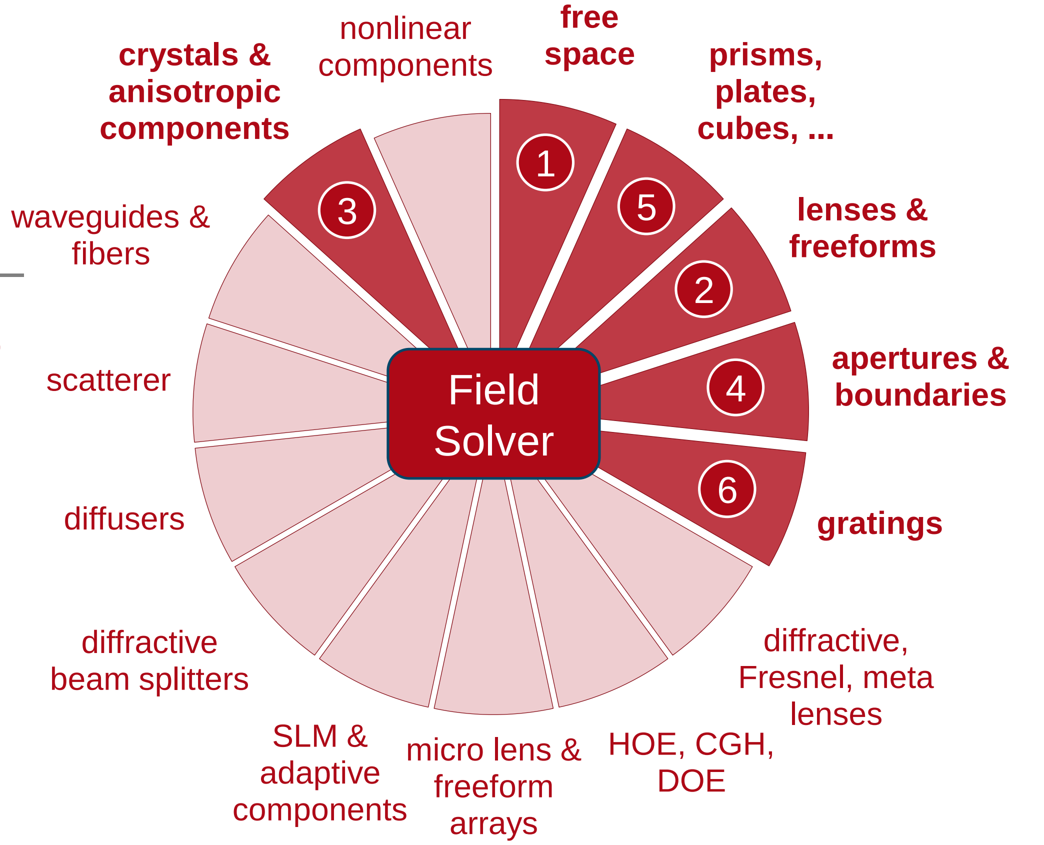

- **Tearing:** optical system decomposed into regions, where specialized regional solvers, which
  - do NOT introduce any physical restrictions
  - may use mathematical approximations

  are applied
- **Interconnection:** solvers per region are connected by fulfilling boundary conditions

Field Tracing Operators

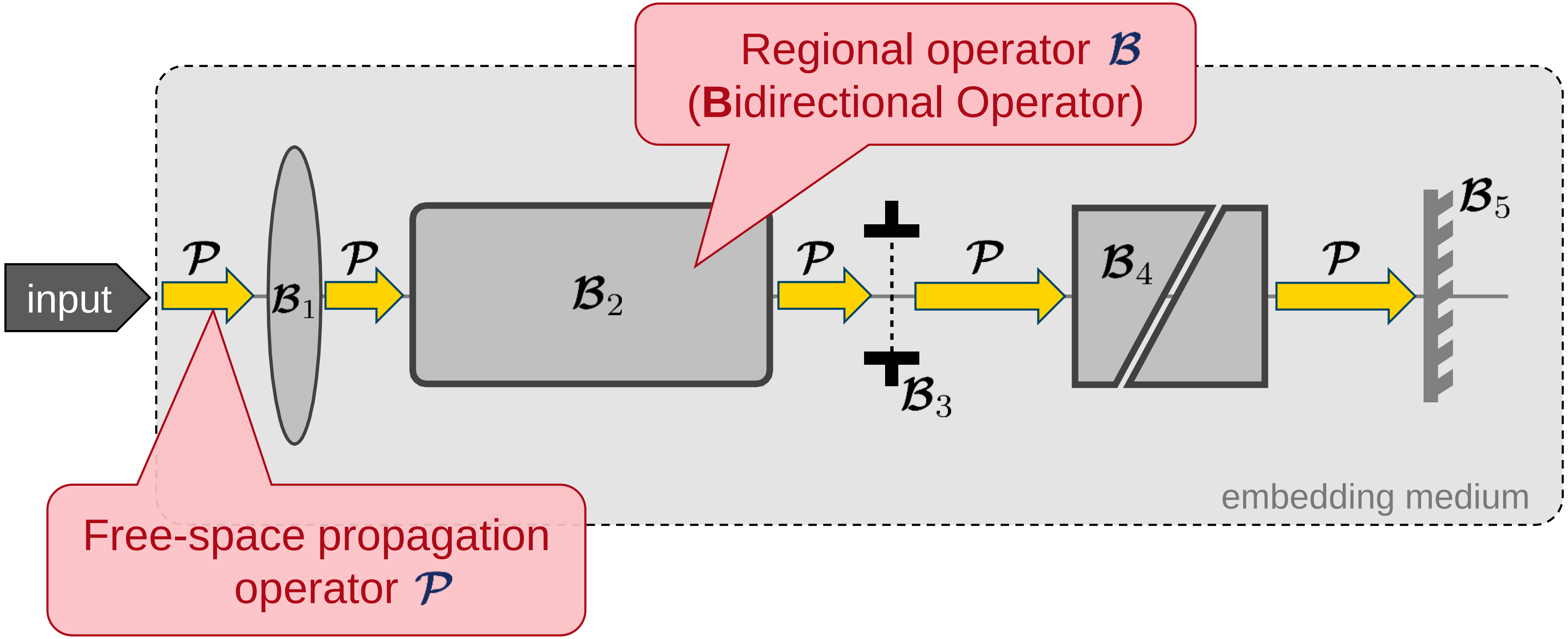

Characterization of Optical Anisotropy

- Constitutive relation

D. W. Berreman, "Optics in Stratified and Anisotropic Media: 4x4-Matrix Formulation," J. Opt. Soc. Am. **62**, 502-510 (1972)

  – Relating the $\boldsymbol{E}/\boldsymbol{H}$-fields and $\boldsymbol{D}/\boldsymbol{B}$-fields

$$\begin{pmatrix} D_x \\ D_y \\ D_z \\ B_x \\ B_y \\ B_z \end{pmatrix} = \begin{pmatrix} \epsilon_{11} & \epsilon_{12} & \epsilon_{13} & 0 & 0 & 0 \\ \epsilon_{21} & \epsilon_{22} & \epsilon_{23} & 0 & 0 & 0 \\ \epsilon_{31} & \epsilon_{32} & \epsilon_{33} & 0 & 0 & 0 \\ 0 & 0 & 0 & \mu_{11} & \mu_{12} & \mu_{13} \\ 0 & 0 & 0 & \mu_{21} & \mu_{22} & \mu_{23} \\ 0 & 0 & 0 & \mu_{31} & \mu_{32} & \mu_{33} \end{pmatrix} \begin{pmatrix} E_x \\ E_y \\ E_z \\ H_x \\ H_y \\ H_z \end{pmatrix}$$

$$= \begin{pmatrix} \underline{\boldsymbol{\epsilon}} & \underline{\boldsymbol{0}} \\ \underline{\boldsymbol{0}} & \underline{\boldsymbol{\mu}} \end{pmatrix}$$

  with the permittivity tensor $\underline{\boldsymbol{\epsilon}}$, permeability tensor $\underline{\boldsymbol{\mu}}$

  – We neglect optical-rotation tensor $\underline{\boldsymbol{\rho}}$ here; but there is not limitation to include it

Maxwell's Equations for Anisotropic Media

- Field equations in matrix form

$$\frac{\mathrm{d}}{\mathrm{d}z}\begin{pmatrix}\tilde{E}_x(\boldsymbol{\kappa},z)\\ \tilde{E}_y(\boldsymbol{\kappa},z)\\ \tilde{H}_x(\boldsymbol{\kappa},z)\\ \tilde{H}_y(\boldsymbol{\kappa},z)\end{pmatrix} = \mathrm{i}k_0\begin{pmatrix}\tilde{\Omega}_{11}(\boldsymbol{\kappa}) & \tilde{\Omega}_{12}(\boldsymbol{\kappa}) & \tilde{\Omega}_{13}(\boldsymbol{\kappa}) & \tilde{\Omega}_{14}(\boldsymbol{\kappa})\\ \tilde{\Omega}_{21}(\boldsymbol{\kappa}) & \tilde{\Omega}_{22}(\boldsymbol{\kappa}) & \tilde{\Omega}_{23}(\boldsymbol{\kappa}) & \tilde{\Omega}_{24}(\boldsymbol{\kappa})\\ \tilde{\Omega}_{31}(\boldsymbol{\kappa}) & \tilde{\Omega}_{32}(\boldsymbol{\kappa}) & \tilde{\Omega}_{33}(\boldsymbol{\kappa}) & \tilde{\Omega}_{34}(\boldsymbol{\kappa})\\ \tilde{\Omega}_{41}(\boldsymbol{\kappa}) & \tilde{\Omega}_{42}(\boldsymbol{\kappa}) & \tilde{\Omega}_{43}(\boldsymbol{\kappa}) & \tilde{\Omega}_{44}(\boldsymbol{\kappa})\end{pmatrix}\begin{pmatrix}\tilde{E}_x(\boldsymbol{\kappa},z)\\ \tilde{E}_y(\boldsymbol{\kappa},z)\\ \tilde{H}_x(\boldsymbol{\kappa},z)\\ \tilde{H}_y(\boldsymbol{\kappa},z)\end{pmatrix}$$

- An ordinary differential equation below

$$\frac{\mathrm{d}}{\mathrm{d}z}f(z) = af(z)$$

has solution in the general form of

$$f(z) = C\exp(\gamma z)$$

Substitution into the field equations …

Maxwell's Equations for Anisotropic Media

- Field equations in matrix form

$$\frac{\mathrm{d}}{\mathrm{d}z}\begin{pmatrix}\tilde{E}_x\\ \tilde{E}_y\\ \tilde{H}_x\\ \tilde{H}_y\end{pmatrix} = \mathrm{i}k_0\begin{pmatrix}\tilde{\Omega}_{11} & \tilde{\Omega}_{12} & \tilde{\Omega}_{13} & \tilde{\Omega}_{14}\\ \tilde{\Omega}_{21} & \tilde{\Omega}_{22} & \tilde{\Omega}_{23} & \tilde{\Omega}_{24}\\ \tilde{\Omega}_{31} & \tilde{\Omega}_{32} & \tilde{\Omega}_{33} & \tilde{\Omega}_{34}\\ \tilde{\Omega}_{41} & \tilde{\Omega}_{42} & \tilde{\Omega}_{43} & \tilde{\Omega}_{44}\end{pmatrix}\begin{pmatrix}\tilde{E}_x\\ \tilde{E}_y\\ \tilde{H}_x\\ \tilde{H}_y\end{pmatrix}$$

- Field solutions

eigenvectors

eigenvalues

$$\begin{pmatrix}\tilde{E}_x\\ \tilde{E}_y\\ \tilde{H}_x\\ \tilde{H}_y\end{pmatrix} = \begin{pmatrix}\tilde{W}^{\mathsf{I}}_{1,+} & \tilde{W}^{\mathsf{II}}_{1,+} & \tilde{W}^{\mathsf{I}}_{1,-} & \tilde{W}^{\mathsf{II}}_{1,-}\\ \tilde{W}^{\mathsf{I}}_{2,+} & \tilde{W}^{\mathsf{II}}_{2,+} & \tilde{W}^{\mathsf{I}}_{2,-} & \tilde{W}^{\mathsf{II}}_{2,-}\\ \tilde{W}^{\mathsf{I}}_{3,+} & \tilde{W}^{\mathsf{II}}_{3,+} & \tilde{W}^{\mathsf{I}}_{3,-} & \tilde{W}^{\mathsf{II}}_{3,-}\\ \tilde{W}^{\mathsf{I}}_{4,+} & \tilde{W}^{\mathsf{II}}_{4,+} & \tilde{W}^{\mathsf{I}}_{4,-} & \tilde{W}^{\mathsf{II}}_{4,-}\end{pmatrix}\begin{pmatrix}e^{\mathrm{i}k^{\mathsf{I}}_{z+}z} & 0 & 0 & 0\\ 0 & e^{\mathrm{i}k^{\mathsf{II}}_{z+}z} & 0 & 0\\ 0 & 0 & e^{\mathrm{i}k^{\mathsf{I}}_{z-}z} & 0\\ 0 & 0 & 0 & e^{\mathrm{i}k^{\mathsf{II}}_{z-}z}\end{pmatrix}\begin{pmatrix}\tilde{C}^{\mathsf{I}}_{+}\\ \tilde{C}^{\mathsf{II}}_{+}\\ \tilde{C}^{\mathsf{I}}_{-}\\ \tilde{C}^{\mathsf{II}}_{-}\end{pmatrix}$$

Maxwell's Equations for Anisotropic Media

- Field equations in matrix form

$$\frac{\mathrm{d}}{\mathrm{d}z}\begin{pmatrix}\tilde{E}_x\\ \tilde{E}_y\\ \tilde{H}_x\\ \tilde{H}_y\end{pmatrix} = \mathrm{i}k_0\begin{pmatrix}\tilde{\Omega}_{11} & \tilde{\Omega}_{12} & \tilde{\Omega}_{13} & \tilde{\Omega}_{14}\\ \tilde{\Omega}_{21} & \tilde{\Omega}_{22} & \tilde{\Omega}_{23} & \tilde{\Omega}_{24}\\ \tilde{\Omega}_{31} & \tilde{\Omega}_{32} & \tilde{\Omega}_{33} & \tilde{\Omega}_{34}\\ \tilde{\Omega}_{41} & \tilde{\Omega}_{42} & \tilde{\Omega}_{43} & \tilde{\Omega}_{44}\end{pmatrix}\ldots$$

Solution by standard linear algebra methods
(matrix diagonalization / eigen-decomposition)

- Field solutions

eigenvectors

eigenvalues

$$\begin{pmatrix}\tilde{E}_x\\ \tilde{E}_y\\ \tilde{H}_x\\ \tilde{H}_y\end{pmatrix} = \begin{pmatrix}\tilde{W}^{\mathsf{I}}_{1,+} & \tilde{W}^{\mathsf{II}}_{1,+} & \tilde{W}^{\mathsf{I}}_{1,-} & \tilde{W}^{\mathsf{II}}_{1,-}\\ \tilde{W}^{\mathsf{I}}_{2,+} & \tilde{W}^{\mathsf{II}}_{2,+} & \tilde{W}^{\mathsf{I}}_{2,-} & \tilde{W}^{\mathsf{II}}_{2,-}\\ \tilde{W}^{\mathsf{I}}_{3,+} & \tilde{W}^{\mathsf{II}}_{3,+} & \tilde{W}^{\mathsf{I}}_{3,-} & \tilde{W}^{\mathsf{II}}_{3,-}\\ \tilde{W}^{\mathsf{I}}_{4,+} & \tilde{W}^{\mathsf{II}}_{4,+} & \tilde{W}^{\mathsf{I}}_{4,-} & \tilde{W}^{\mathsf{II}}_{4,-}\end{pmatrix}\begin{pmatrix}e^{ik^{\mathsf{I}}_{z+}z} & 0 & 0 & 0\\ 0 & e^{ik^{\mathsf{II}}_{z+}z} & 0 & 0\\ 0 & 0 & e^{ik^{\mathsf{I}}_{z-}z} & 0\\ 0 & 0 & 0 & e^{ik^{\mathsf{II}}_{z-}z}\end{pmatrix}\begin{pmatrix}\tilde{C}^{\mathsf{I}}_{+}\\ \tilde{C}^{\mathsf{II}}_{+}\\ \tilde{C}^{\mathsf{I}}_{-}\\ \tilde{C}^{\mathsf{II}}_{-}\end{pmatrix}$$

Intrinsic properties of field in anisotropic media

Example: Polarization Conversion in Calcite

input field

- Fundamental Gaussian
- Wavelength 633 nm
- Diameter 3 mm
- Linearly polarized along *x* direction

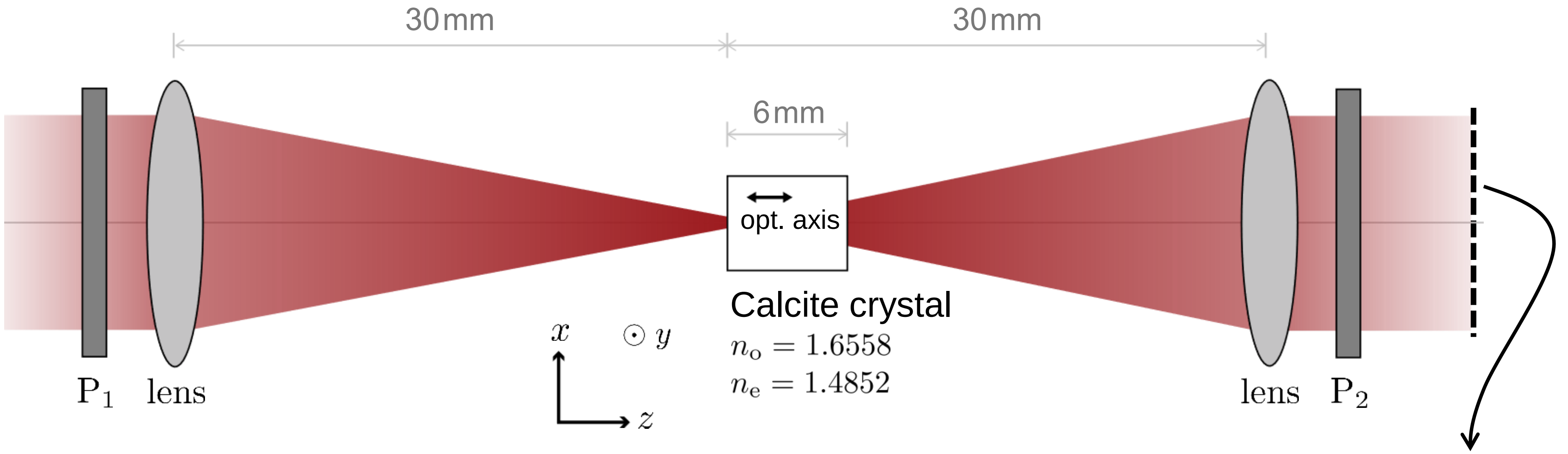

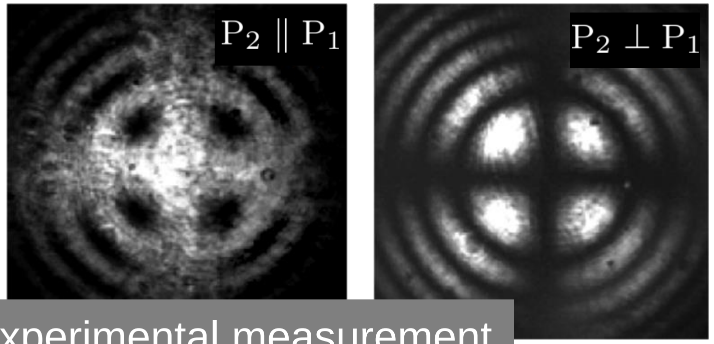

Experimental measurement from reference

Izdebskaya *et al*., “Dynamics of linear polarization conversion in uniaxial crystals,” Opt. Express **17**, 18196-18208 (2009)

Example: Polarization Conversion in Calcite

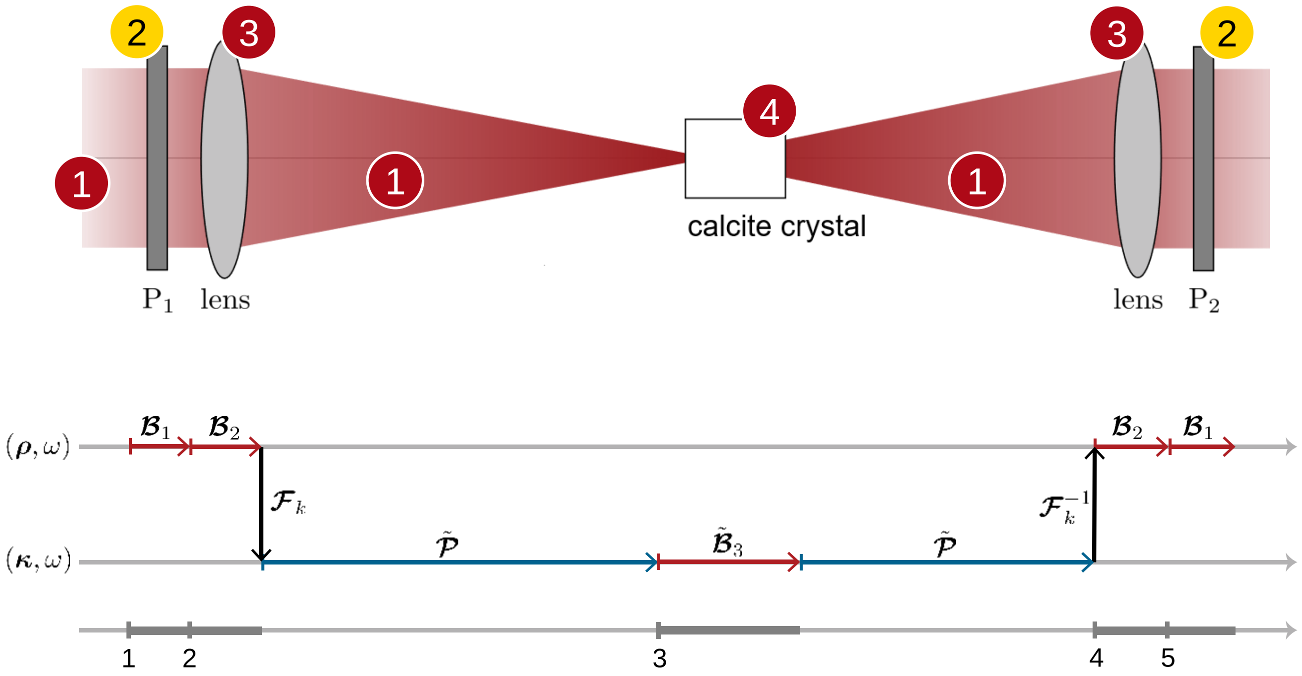

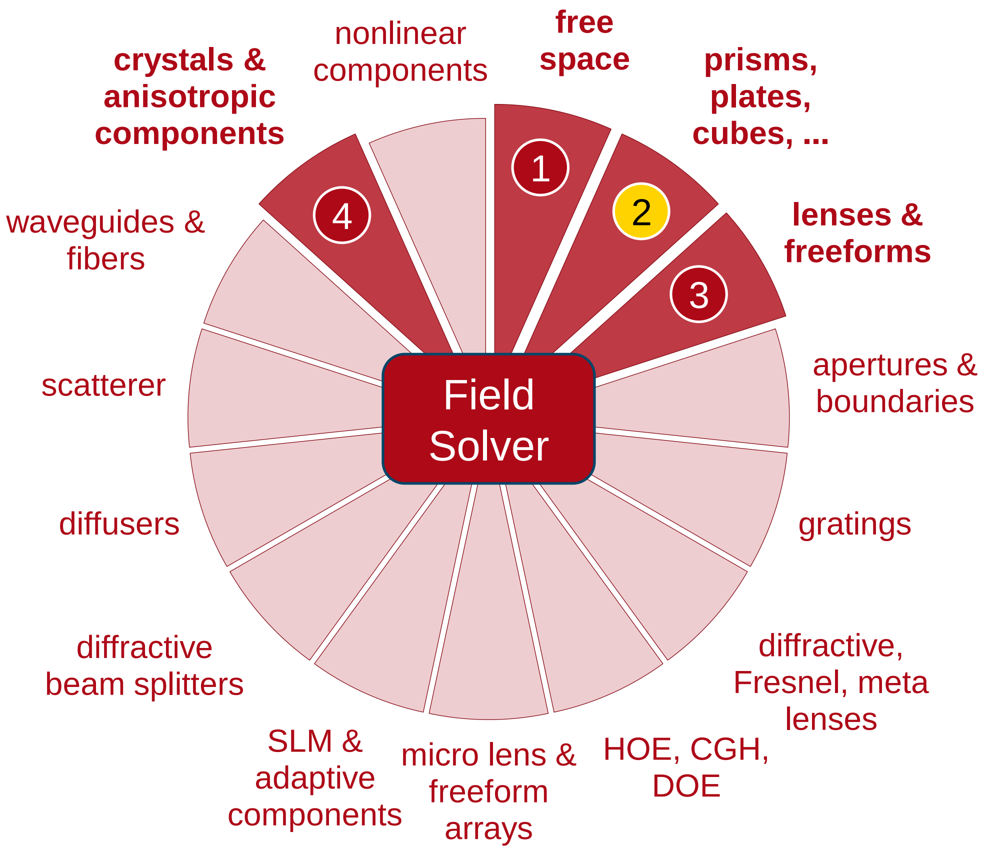

Idealized component

Example: Polarization Conversion in Calcite

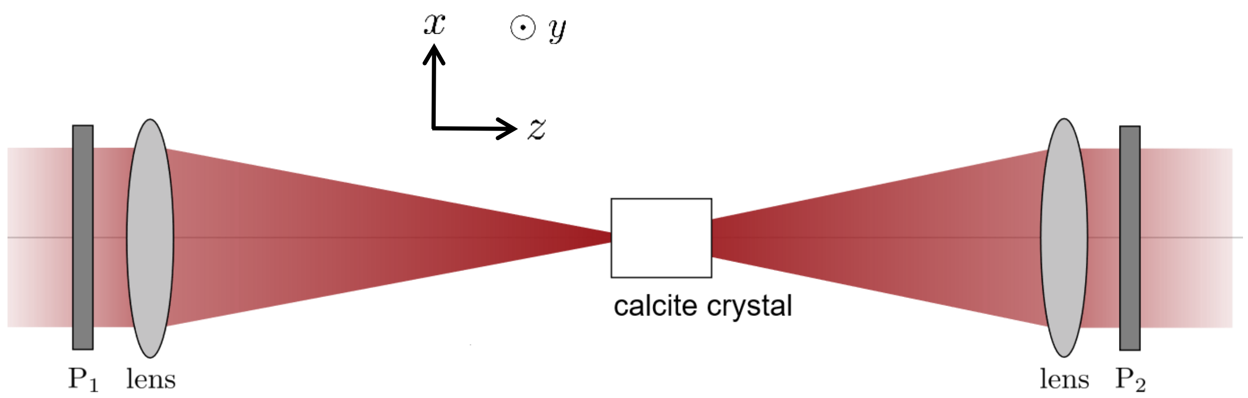

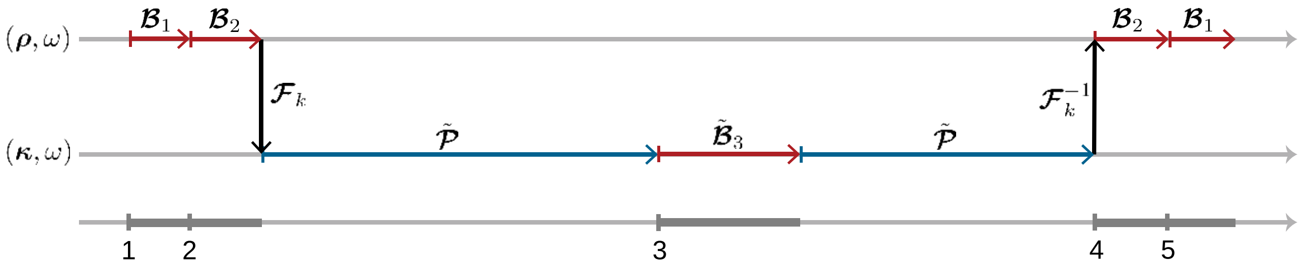

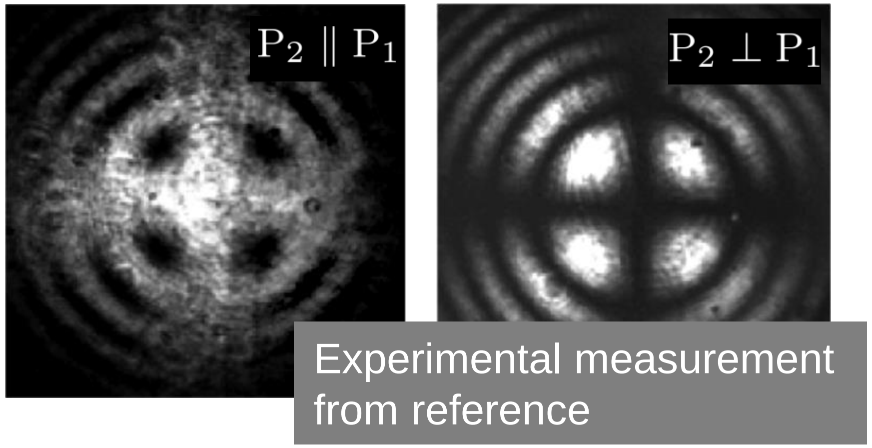

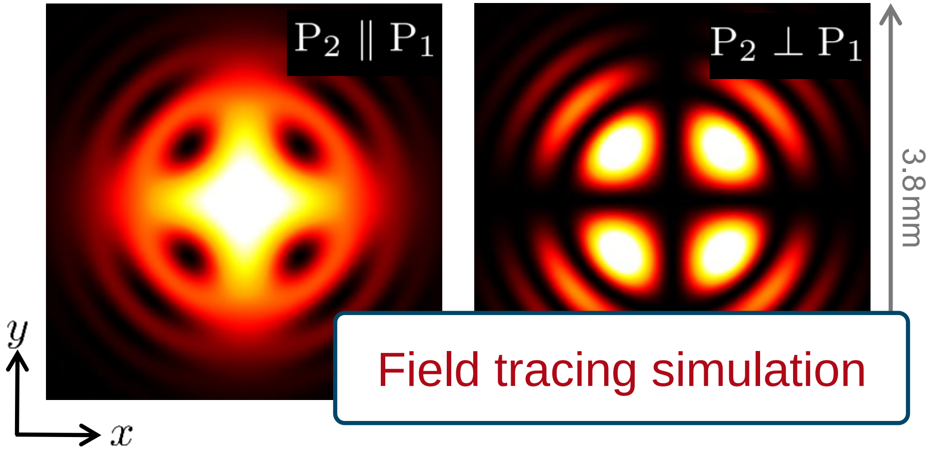

Example: Polarization Conversion in Calcite

Simulation time ~12 seconds
(Intel Core i7-4910MQ @2.9GHz)

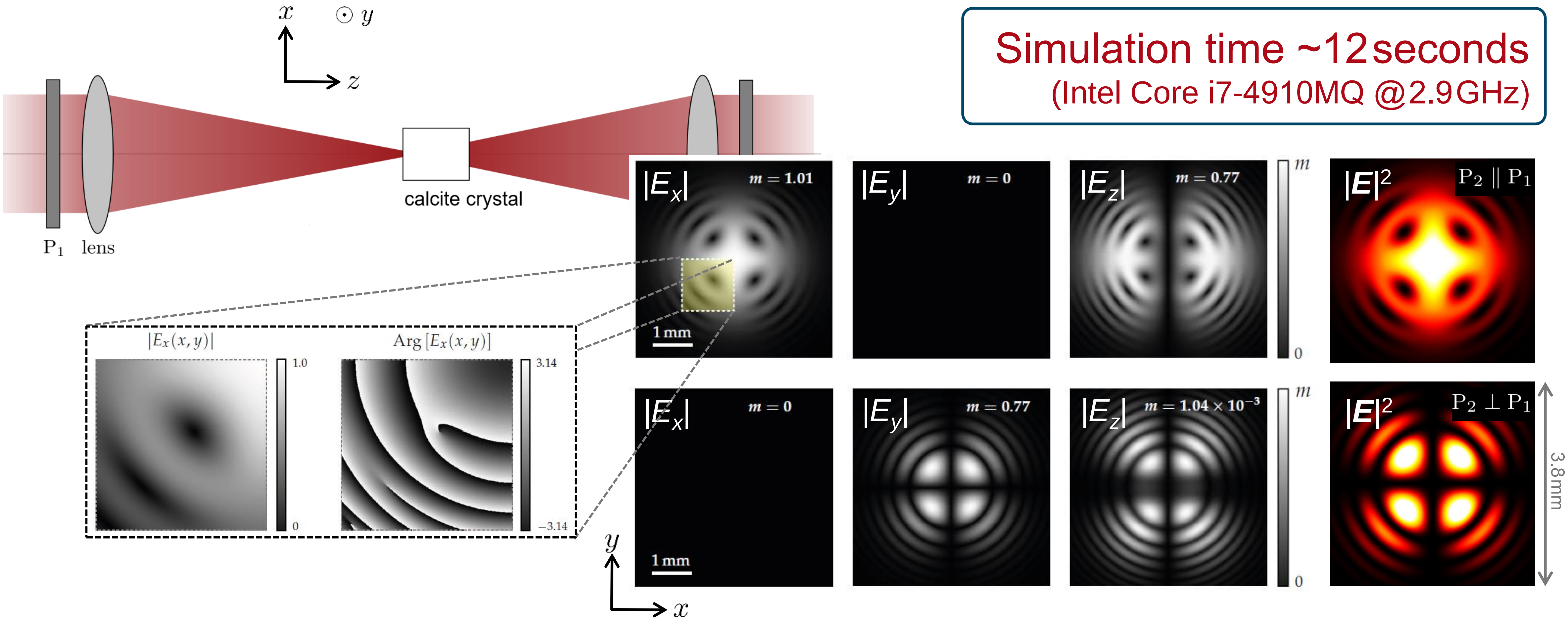

Extended Applications

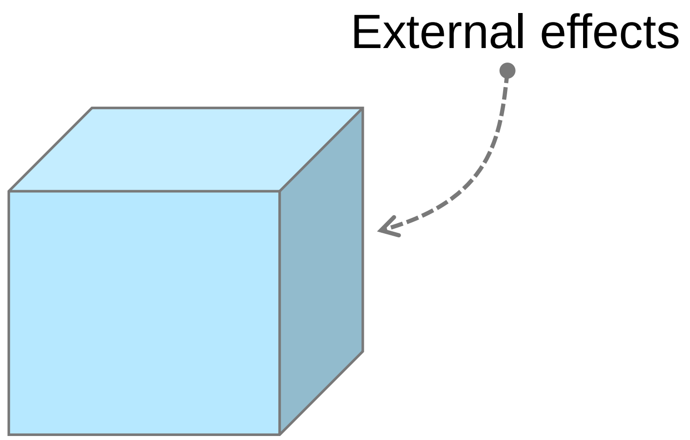

$$\begin{pmatrix} \epsilon & 0 & 0 \\ 0 & \epsilon & 0 \\ 0 & 0 & \epsilon \end{pmatrix} \rightarrow \begin{pmatrix} \epsilon_{11} & \epsilon_{12} & \epsilon_{13} \\ \epsilon_{21} & \epsilon_{22} & \epsilon_{23} \\ \epsilon_{31} & \epsilon_{32} & \epsilon_{33} \end{pmatrix}$$

Induced birefringence

Laser Crystal Packaging and Stress-Induced Birefringence

- Solderjet bumping technique
  - high mechanical strength and stability
  - hermetical sealing and vacuum compatibility
  - radiation resistance
  - miniaturization and sub-µm precision

P. Ribes-Pleguezuelo, S. Zhang, E. Beckert, R. Eberhardt, F. Wyrowski, and A. Tünnermann, “Method to simulate and analyse induced stresses for laser crystal packaging technologies,” Opt. Express **25**, 5927-5940 (2017)

How does induced birefringence affect the polarization?

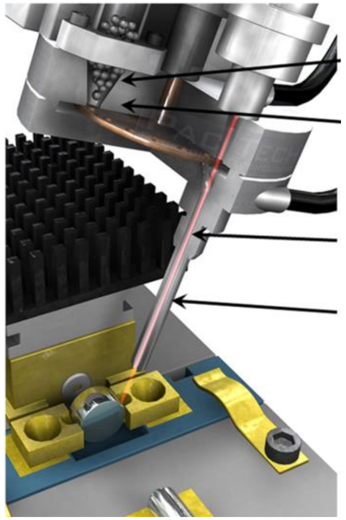

solderjet bumping technique
(pictures from Frauenhofer IOF)

Stress-Induced Birefringence

- Stress-induced birefringence
  - relation between stress and optical permittivity

finite-element method (FEM) analysis

ANSYS

stress tensor

$$\begin{pmatrix} \sigma_1 & \sigma_6 & \sigma_5 \\ \sigma_6 & \sigma_2 & \sigma_4 \\ \sigma_5 & \sigma_4 & \sigma_3 \end{pmatrix}$$

piezo-optic constant

$$\Delta B_m = \pi_{mn} \sigma_n$$

changes in impermeability tensor

$$\begin{pmatrix} \Delta B_1 & \Delta B_6 & \Delta B_5 \\ \Delta B_6 & \Delta B_2 & \Delta B_4 \\ \Delta B_5 & \Delta B_4 & \Delta B_3 \end{pmatrix}$$

$$B_m = B_{0,m} + \Delta B_m$$

stress-free values

(related to refractive index/indicies)

impermeability tensor

$$\begin{pmatrix} B_1 & B_6 & B_5 \\ B_6 & B_2 & B_4 \\ B_5 & B_4 & B_3 \end{pmatrix}$$

$$[\epsilon_{ij}]^{-1} = [B_{ij}]$$

permittivity tensor

$$\begin{pmatrix} \epsilon_1 & \epsilon_6 & \epsilon_5 \\ \epsilon_6 & \epsilon_2 & \epsilon_4 \\ \epsilon_5 & \epsilon_4 & \epsilon_3 \end{pmatrix}$$

subsequent optical simulation

Stress-Induced Birefringence

- Input field

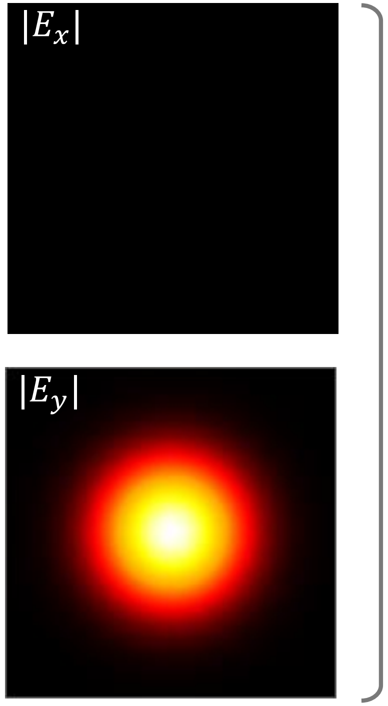

- Wavelength 1064 nm
- Fundamental Gaussian
- Waist diameter 100 µm

- YAG crystal

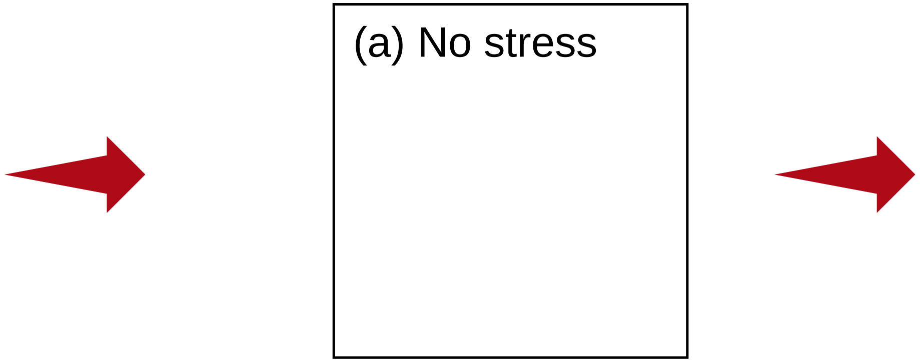

- Output field

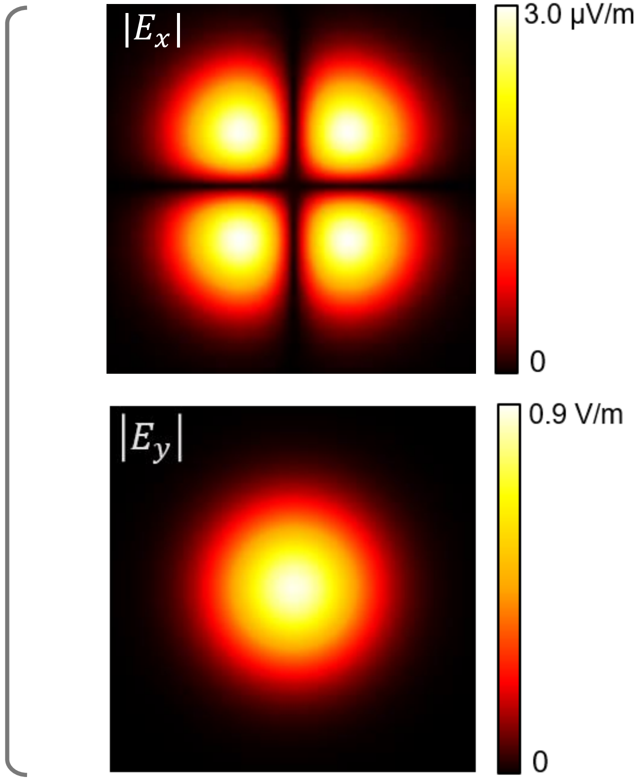

Stress-Induced Birefringence

- Input field

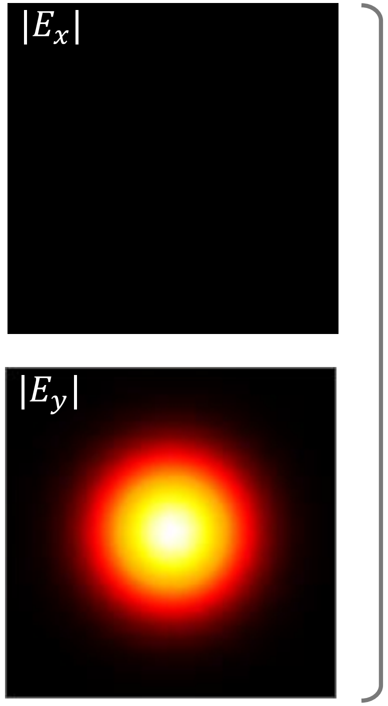

- Wavelength 1064 nm
- Fundamental Gaussian
- Waist diameter 100 µm

- YAG crystal

(b) Test stress

- Output field

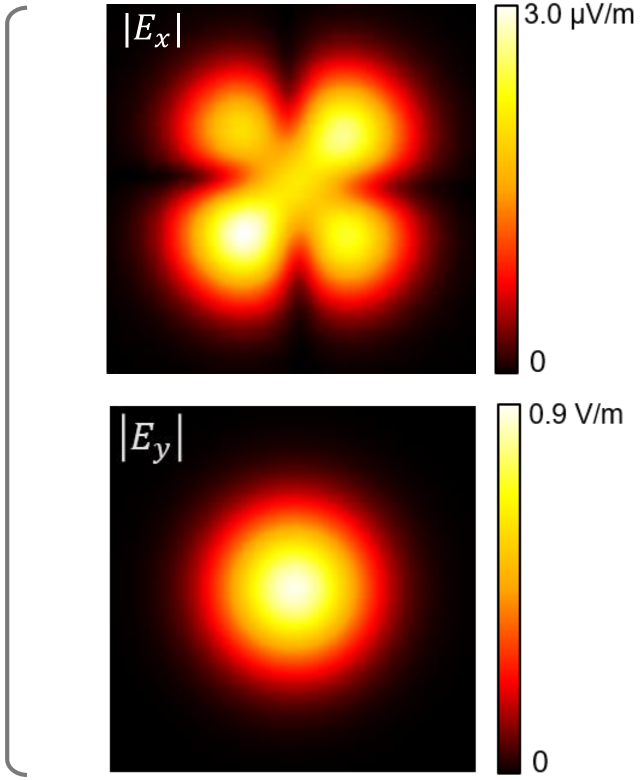

Stress-Induced Birefringence

- Input field

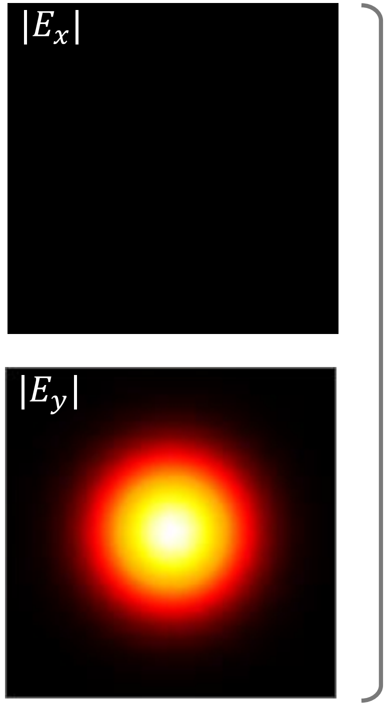

- Wavelength 1064 nm
- Fundamental Gaussian
- Waist diameter 100 µm

- YAG crystal

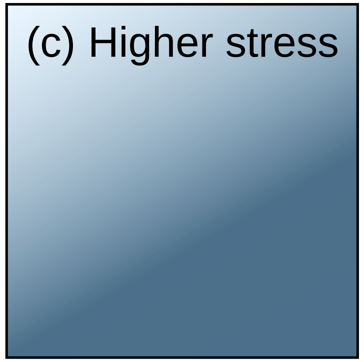

- Output field

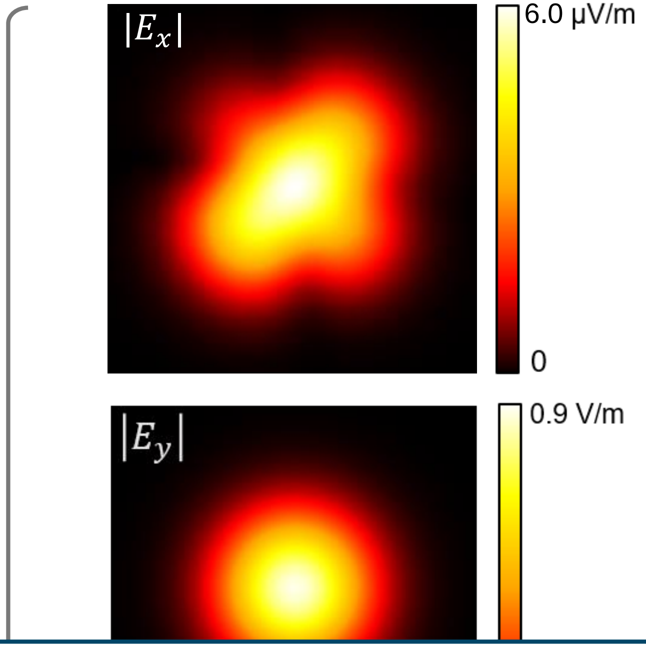

Simulation time ~4 seconds per case
(Intel Core i7-4910MQ @2.9GHz)

Idealized Model for Anisotropic Components

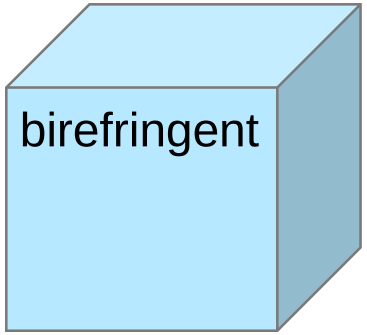

$$\begin{pmatrix} \epsilon_{11} & \epsilon_{12} & \epsilon_{13} \\ \epsilon_{21} & \epsilon_{22} & \epsilon_{23} \\ \epsilon_{31} & \epsilon_{32} & \epsilon_{33} \end{pmatrix} \; ?$$

material property
not available

Polarizer in Non-Paraxial Situation

S. Zhang, H. Partanen, C. Hellmann, and F. Wyrowski, “Non-paraxial idealized polarizer model,” Opt. Express 26, 9840-9849 (2018)

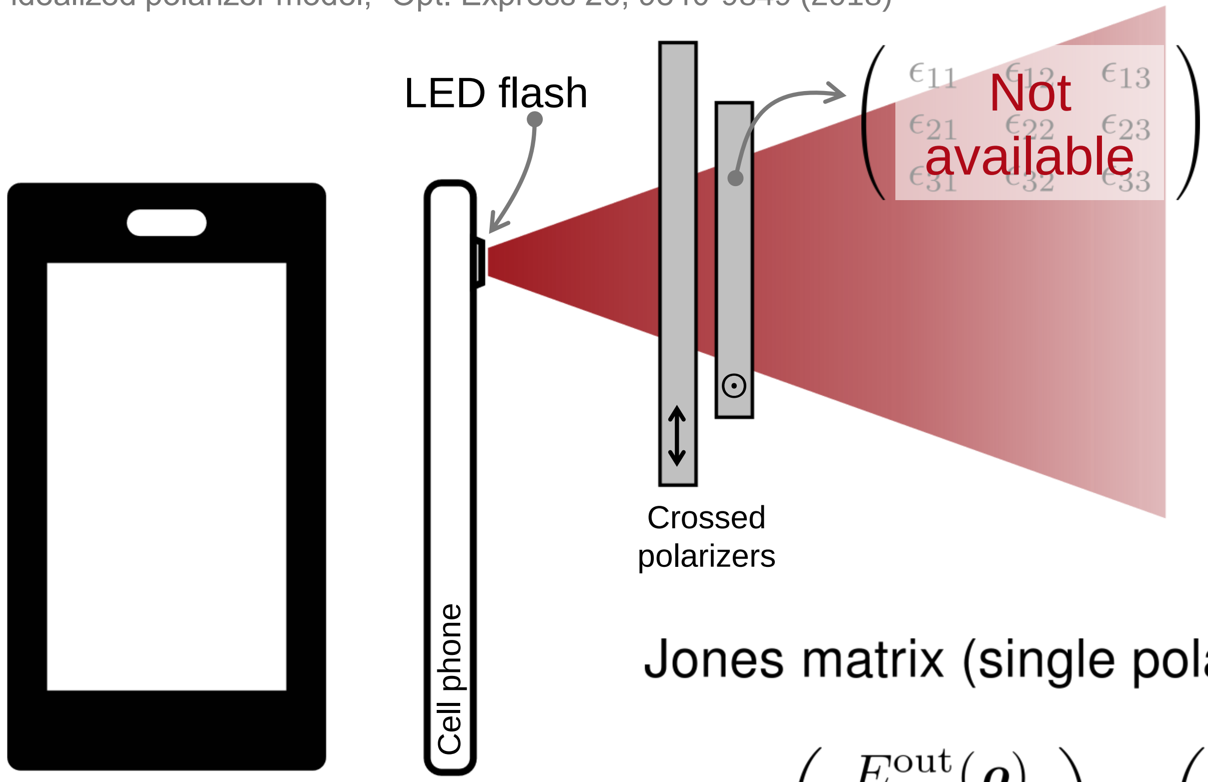

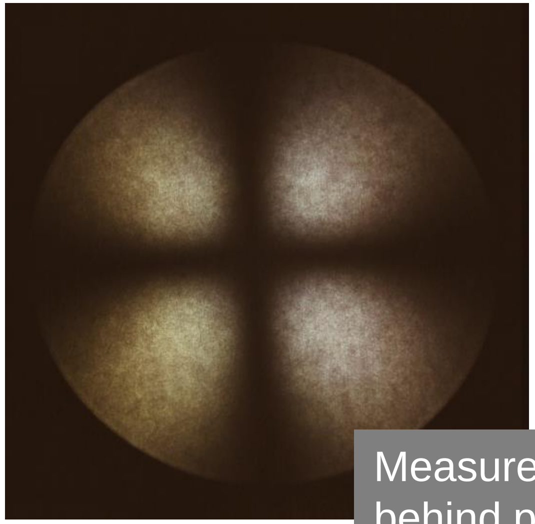

Measurement on paper behind polarizers

Jones matrix (single polarizer in x)

$$\begin{pmatrix} E_x^{\mathrm{out}}(\boldsymbol{\rho}) \\ E_y^{\mathrm{out}}(\boldsymbol{\rho}) \end{pmatrix} = \begin{pmatrix} 1 & 0 \\ 0 & 0 \end{pmatrix} \begin{pmatrix} E_x^{\mathrm{in}}(\boldsymbol{\rho}) \\ E_y^{\mathrm{in}}(\boldsymbol{\rho}) \end{pmatrix}$$

Polarizer in Non-Paraxial Situation

S. Zhang, H. Partanen, C. Hellmann, and F. Wyrowski, "Non-paraxial idealized polarizer model," Opt. Express 26, 9840-9849 (2018)

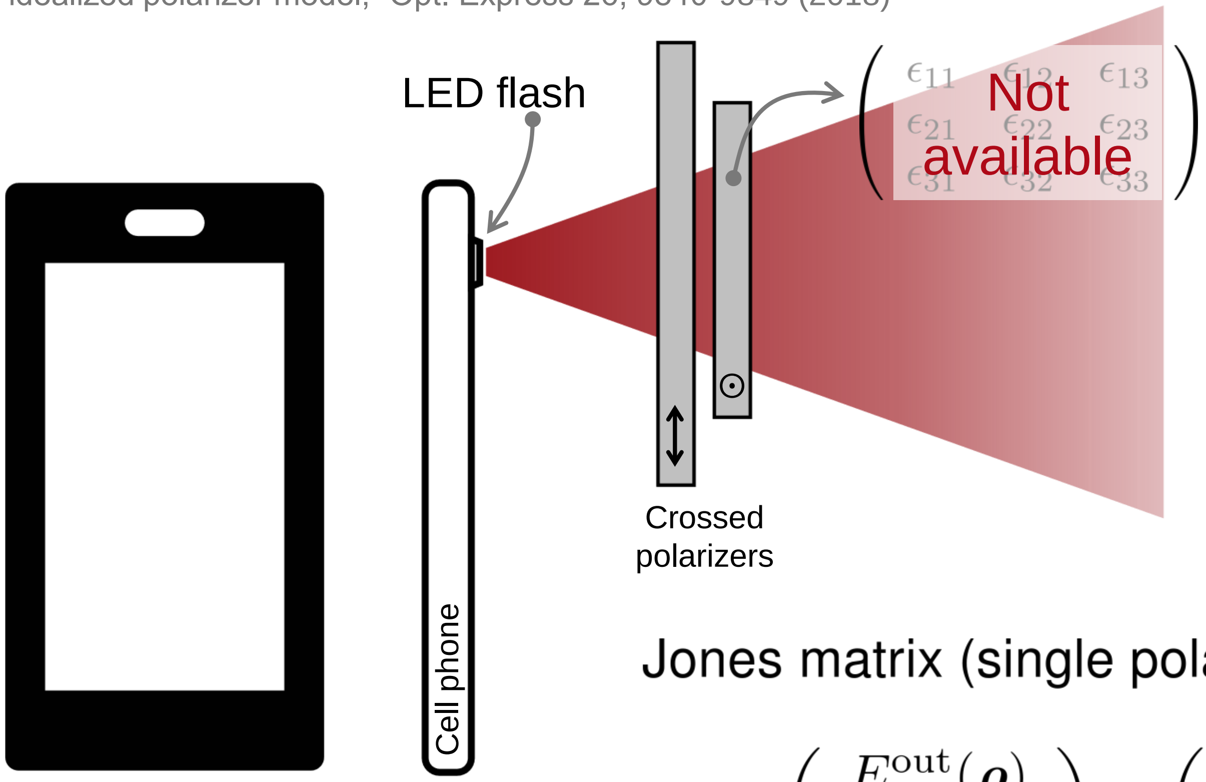

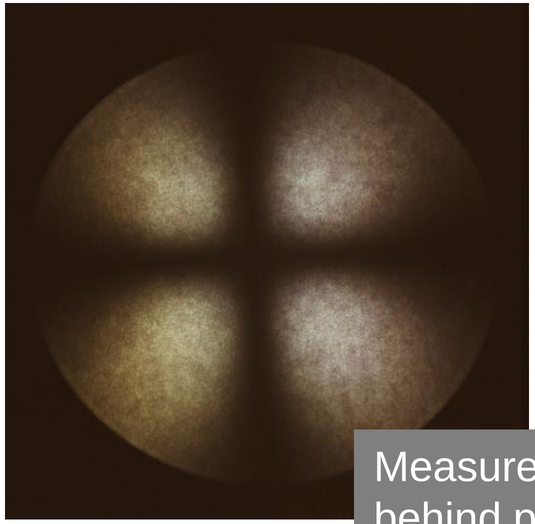

Measurement on paper behind polarizers

Jones matrix (single polarizer in y)

$$\begin{pmatrix} E_x^{\text{out}}(\boldsymbol{\rho}) \\ E_y^{\text{out}}(\boldsymbol{\rho}) \end{pmatrix} = \begin{pmatrix} 0 & 0 \\ 0 & 1 \end{pmatrix} \begin{pmatrix} E_x^{\text{in}}(\boldsymbol{\rho}) \\ E_y^{\text{in}}(\boldsymbol{\rho}) \end{pmatrix}$$

Polarizer in Non-Paraxial Situation

S. Zhang, H. Partanen, C. Hellmann, and F. Wyrowski, “Non-paraxial idealized polarizer model,” Opt. Express 26, 9840-9849 (2018)

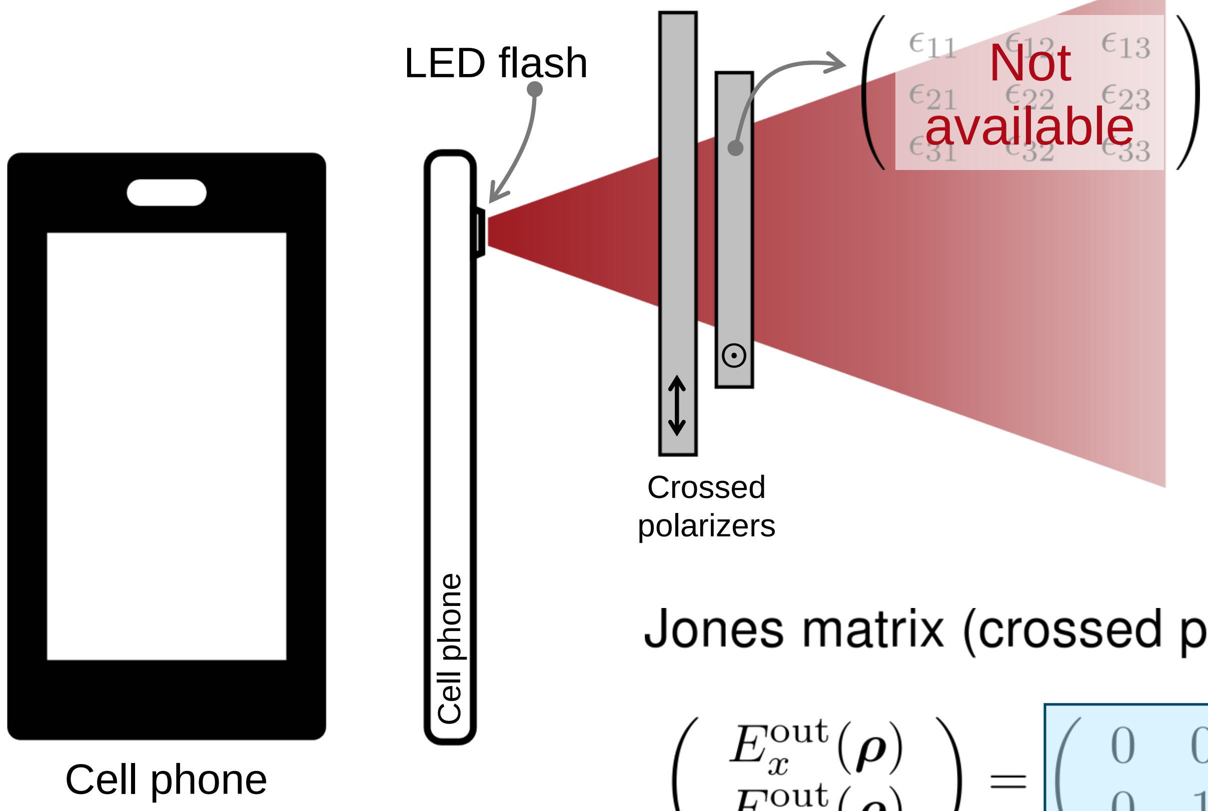

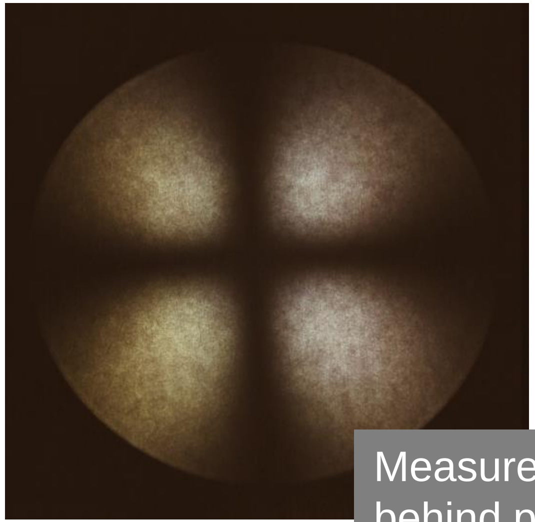

Measurement on paper behind polarizers

Jones matrix (crossed polarizers)

$$\begin{pmatrix} E_x^{\mathrm{out}}(\boldsymbol{\rho}) \\ E_y^{\mathrm{out}}(\boldsymbol{\rho}) \end{pmatrix} = \begin{pmatrix} 0 & 0 \\ 0 & 1 \end{pmatrix} \begin{pmatrix} 1 & 0 \\ 0 & 0 \end{pmatrix} \begin{pmatrix} E_x^{\mathrm{in}}(\boldsymbol{\rho}) \\ E_y^{\mathrm{in}}(\boldsymbol{\rho}) \end{pmatrix}$$

Polarizer in Non-Paraxial Situation

- Field solution in polarizer plate

$$\begin{pmatrix} \tilde{E}_x \\ \tilde{E}_y \\ \tilde{H}_x \\ \tilde{H}_y \end{pmatrix} = \begin{pmatrix} 1 & 0 & 1 & 0 \\ \tilde{W}_B & \tilde{W}_D & \tilde{W}_B & -\tilde{W}_D \\ 0 & 1 & 0 & 1 \\ \tilde{W}_C & \tilde{W}_B & -\tilde{W}_C & \tilde{W}_B \end{pmatrix} \begin{pmatrix} \tilde{C}_{\mathrm{TM}+} \exp(\mathrm{i}k_z^{\mathrm{TM}} z) \\ \tilde{C}_{\mathrm{TE}+} \exp(\mathrm{i}k_z^{\mathrm{TE}} z) \\ \tilde{C}_{\mathrm{TM}-} \exp(-\mathrm{i}k_z^{\mathrm{TM}} z) \\ \tilde{C}_{\mathrm{TE}-} \exp(-\mathrm{i}k_z^{\mathrm{TE}} z) \end{pmatrix}$$

- Mode propagation through polarizer

$$\begin{pmatrix} \tilde{C}_{\mathrm{TM}}^{\mathrm{out}} \\ \tilde{C}_{\mathrm{TE}}^{\mathrm{out}} \end{pmatrix} = \begin{pmatrix} 0 & 0 \\ 0 & 1 \end{pmatrix} \begin{pmatrix} \tilde{C}_{\mathrm{TM}}^{\mathrm{in}} \\ \tilde{C}_{\mathrm{TE}}^{\mathrm{in}} \end{pmatrix}$$

- Conversion to field components

$$\begin{pmatrix} \tilde{E}_x^{\mathrm{out}}(\boldsymbol{\kappa}) \\ \tilde{E}_y^{\mathrm{out}}(\boldsymbol{\kappa}) \end{pmatrix} = \begin{pmatrix} 0 & 0 \\ -\tilde{W}_B(\boldsymbol{\kappa}) & 1 \end{pmatrix} \begin{pmatrix} \tilde{E}_x^{\mathrm{in}}(\boldsymbol{\kappa}) \\ \tilde{E}_y^{\mathrm{in}}(\boldsymbol{\kappa}) \end{pmatrix}$$

$$\tilde{W}_B(\boldsymbol{\kappa}) = \frac{k_x k_y}{-k_0^2 \epsilon + k_x^2}$$

Polarizer

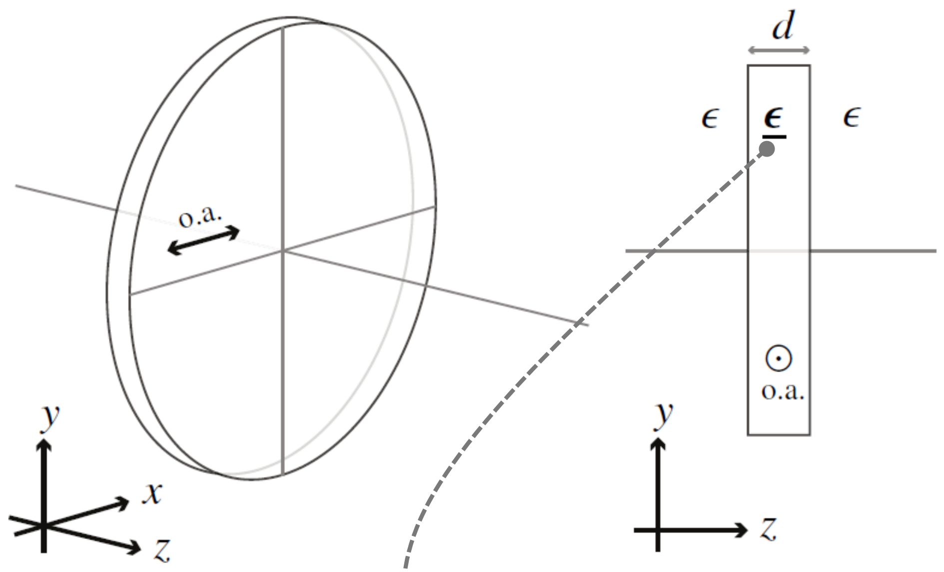

$$\underline{\boldsymbol{\epsilon}} = \begin{pmatrix} \epsilon_{\mathrm{e}} & 0 & 0 \\ 0 & \epsilon_{\mathrm{o}} & 0 \\ 0 & 0 & \epsilon_{\mathrm{o}} \end{pmatrix}$$

Polarizer in Non-Paraxial Situation

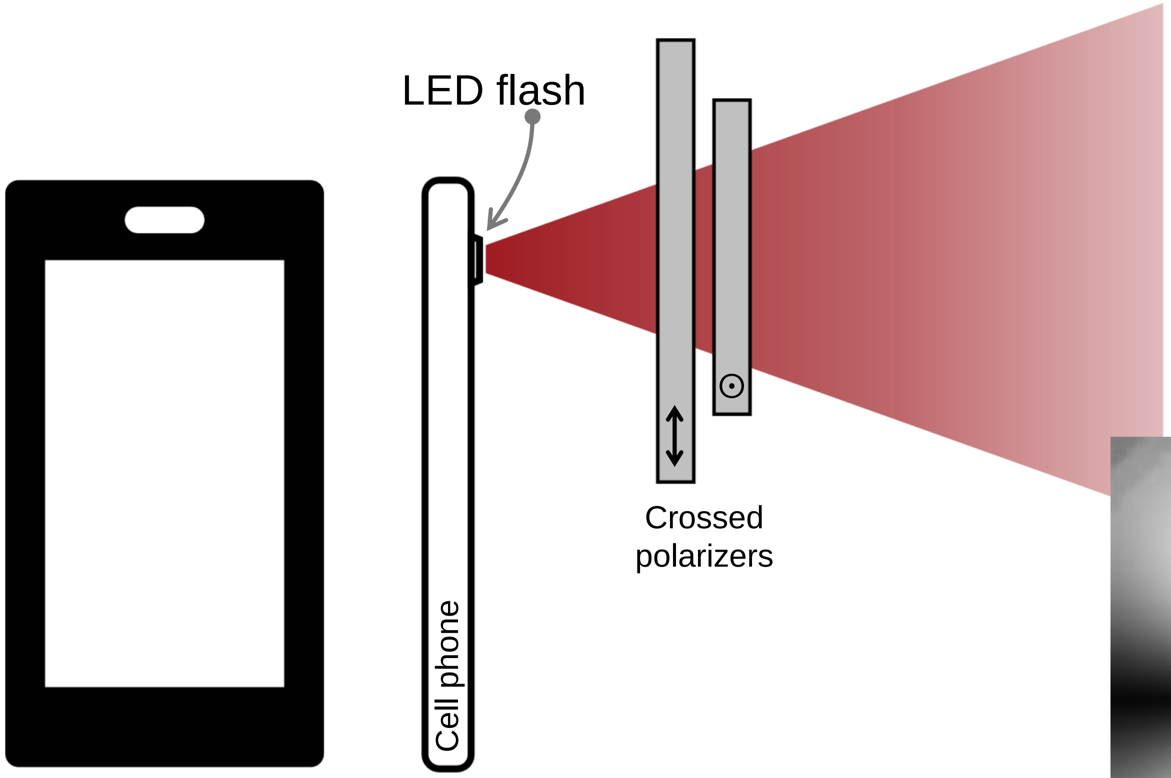

Cell phone

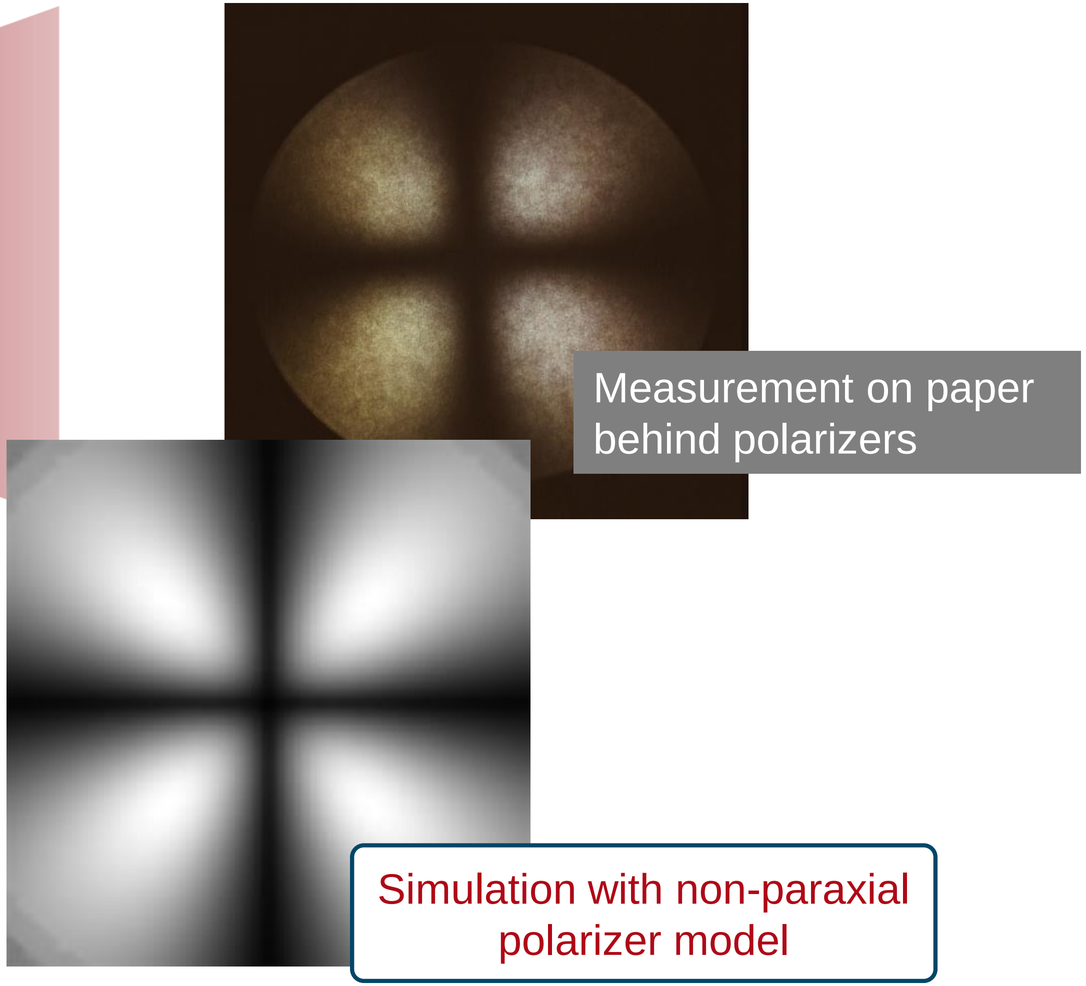

VirtualLab Fusion – Connecting Field Solvers

Booth #110